



Publication Year	2018
Acceptance in OA	2024-03-01T10:21:59Z
Title	Electroplated bismuth absorbers for planar NTD-Ge sensor arrays applied to hard x-ray detection in astrophysics
Authors	FERRUGGIA BONURA, Salvatore, GULLI, DANIELE, BARBERA, Marco, COLLURA, Alfonso, SCIORTINO, LUISA, SPOTO, DOMENICO, TODARO, Michela, PUCCIO, ELENA, MONTINARO, NICOLA, VARISCO, Salvatore, Santamaria, M., Di Franco, F., Maniscalco, A., Zaffora, A., Botta, L., LO CICERO, UGO
Publisher's version (DOI)	10.1117/12.2314195
Handle	http://hdl.handle.net/20.500.12386/34846
Serie	PROCEEDINGS OF SPIE
Volume	10709

PROCEEDINGS OF SPIE

[SPIDigitalLibrary.org/conference-proceedings-of-spie](https://spiedigitallibrary.org/conference-proceedings-of-spie)

Electroplated bismuth absorbers for planar NTD-Ge sensor arrays applied to hard x-ray detection in astrophysics

S. Ferruggia Bonura, D. Gulli, M. Barbera, A. Collura, L. Sciortino, et al.

S. Ferruggia Bonura, D. Gulli, M. Barbera, A. Collura, L. Sciortino, D. Spoto, M. Todaro, E. Puccio, N. Montinaro, S. Varisco, M. Santamaria, F. Di Franco, A. Maniscalco, A. Zaffora, L. Botta, U. Lo Cicero, "Electroplated bismuth absorbers for planar NTD-Ge sensor arrays applied to hard x-ray detection in astrophysics," Proc. SPIE 10709, High Energy, Optical, and Infrared Detectors for Astronomy VIII, 107092D (20 July 2018); doi: 10.1117/12.2314195

SPIE.

Event: SPIE Astronomical Telescopes + Instrumentation, 2018, Austin, Texas, United States

Electroplated bismuth absorbers for planar NTD-Ge sensor arrays applied to hard X-ray detection in astrophysics

S. Ferruggia Bonura^{1,2}, D. Gulli¹, M. Barbera^{2,1}, A. Collura¹, L. Sciortino^{2,1},
D. Spoto^{3,1}, M. Todaro¹, E. Puccio¹, N. Montinaro¹, S. Varisco¹,
M. Santamaria⁴, F. Di Franco⁴, A. Maniscalco⁴, A. Zaffora⁴, L. Botta⁵, and U. Lo Cicero^{1,2}

1: Istituto Nazionale di Astrofisica, Osservatorio Astronomico di Palermo, Palermo – Italy

2: Università degli Studi di Palermo, Dipartimento di Fisica e Chimica, Palermo – Italy

3: Agenzia Spaziale Italiana (ASI) – Roma – Italy

4: Università degli Studi di Palermo, Dipartimento di Ingegneria Civile Ambientale Aerospaziale e dei Materiali, Electrochemical Material Science Laboratory, Palermo – Italy

5: Università degli Studi di Palermo, Dipartimento di Ingegneria Civile Ambientale Aerospaziale e dei Materiali, Palermo - Italy

ABSTRACT

Single sensors or small arrays of manually assembled neutron transmutation doped germanium (NTD-Ge) based microcalorimeters have been widely used as high energy-resolution detectors from infrared to hard X-rays. Several planar technological processes were developed in the last years aimed at the fabrication of NTD-Ge arrays, specifically designed to produce soft X-ray detectors. One of these processes consists in the fabrication of the absorbers. In order to absorb efficiently hard X-ray photons, the absorber has to be properly designed and a suitable material has to be employed. Bismuth offers interesting properties in terms of absorbing capability, of low heat capacity (needed to obtain high energy resolution) and deposition technical feasibility, moreover, it has already been used as absorber for other types of microcalorimeters. Here we present the electroplating process we adopted to grow bismuth absorbers for fabricating planar microcalorimeter arrays for hard X-rays detection. The process was specifically tuned to grow uniform Bi films with thickness up to $\sim 70 \mu\text{m}$. This work is part of a feasibility study for a stratospheric balloon borne experiment that would observe hard X-rays (20-100 keV) from solar corona.

KEYWORDS

Microcalorimeters; NTD-Ge; X-rays; thick film; bismuth; electroplating.

INTRODUCTION

The Sun is surrounded by a very hot (million degrees) atmosphere (the solar corona) consisting of very tenuous optically thin plasma strongly interacting with the magnetic field and emitting X-rays. The magnetic field plays a key role in the heating of the solar corona, but the detailed heating mechanisms are still under investigation. It is well known that non thermal hard X-rays are produced in the solar corona especially during energetic impulsive events (flares)^{1,2,3}, however, these events have never been observed at high energy resolution ($\Delta E < 100 \text{ eV}$). Recently, we have started a feasibility study for a stratospheric balloon experiment, named MISTER-X, aimed at observing hard X-rays from the solar corona in the 20-100 keV energy band, with an energy resolution of the order of $\Delta E = 50 \text{ eV}$, using NTD Ge cryogenic microcalorimeter detectors. Such preliminary feasibility study was funded by the Italian National Institute for Astrophysics (INAF) within an agreement with the Italian Space Agency (ASI).

In this paper, we describe part of the work done to develop the hard X-ray microcalorimeter to be employed in the experiment, and in particular the development of the deposition process employed to build the X-ray absorbers.

This paper is organized as follows: section 1 introduces NTD-Ge microcalorimeters; section 2 illustrates the microcalorimeter X-ray absorber design procedure; section 3 describes the electroplating process; in section 4 shows the results; in section 5 we draw our conclusions and work perspectives.

1. NTD-GE MICROCALORIMETERS

X-ray microcalorimeters are based on the measurement of the temperature increase caused by the interaction of a single particle or photon with the absorber of the detector⁴. Such sensors consist of an absorber in high Z material and a sensitive thermal sensor (thermistor). NTD Ge thermometers, whose electrical resistance presents a high negative temperature coefficient, have been successfully used as thermistors of high sensitive X-ray microcalorimeters operating both at soft^{5,6} and hard⁷ x-rays. NTD Ge is obtained by irradiating high purity Ge crystals with thermal neutrons inside a nuclear reactor^{8,9}.

The general scheme of such a detector¹⁰ is depicted in the following picture (Figure 1):

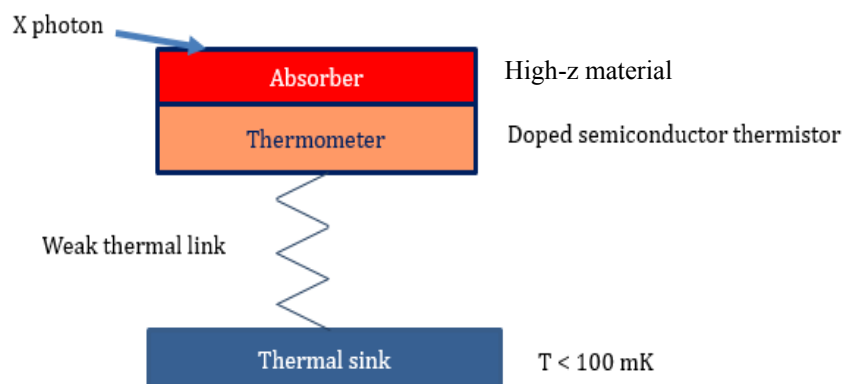


Figure 1 - NTD Ge microcalorimeter schematic.

When a X-ray photon is absorbed, its energy E is transferred to the material whose temperature T increases; such increase ΔT causes a change in the resistance $R(T)$ of the semiconductor thermometer. The measurement of this change provides a measurement of ΔT . A weak thermal link to a thermal sink at cryogenic temperature $T < 100\text{mK}$ brings the temperature back to its steady value, allowing the detection of another photon. If $C_{\text{tot}} = C_{\text{abs}} + C_T$ is the total heat capacity of the device (absorber + thermometer), the temperature increase is:

$$\Delta T = \frac{E}{C_{\text{tot}}}, \quad (1)$$

where E is the energy of the absorbed photon.

The energy resolution (Full Width Half Maximum) of the detector is given by¹¹:

$$\Delta E_{FWHM} \cong 2.355\xi\sqrt{k_B T^2 C_{\text{tot}}} \quad (2)$$

in which ξ is a coefficient accounting for the thermometer sensitivity and k_B is the Boltzmann constant.

2. MICROCALORIMETER X-RAY ABSORBER DESIGN PROCEDURE

The design of the absorbers requires the definition of the following parameters:

- 1) energy band;
- 2) energy resolution ΔE_{FWHM} ;
- 3) quantum efficiency QE;
- 4) operating temperature.

Our group has already experience^{12,13,14} in designing and fabricating NTD-Ge microcalorimeters for soft X-rays (< 10 keV). With our recent research activities, we are aiming to extend the detectable energy band up to 100 keV.

The scientific goal to detect hard X-ray features from the solar corona determines a quantum efficiency requirement of > 0.3 at 60 keV while a lower value can be accepted at higher energies. This QE value has been identified as a good compromise between high QE in a wide part of the energy band, energy resolution (the higher the mass the higher the thermal capacity is and the lower the energy resolution) and technological process development. The baseline for the operating temperature is 50 mK. Design requirements are summarized in table 1.

The quantum efficiency requirement limits the choice to very high Z materials for the absorber (bismuth, gold, tantalum, rhenium, osmium, tin¹⁵). Bismuth offers some advantages due to its high X-ray absorption in a wide spectrum range, low heat capacity, and simple deposition technology (electroplating)^{16,17,18}. For these reasons, it has been identified as the first choice for our work.

Figure 2 shows theoretical QE curves of bismuth absorbers with different thickness in a wide energy range, based on X-ray absorption data¹⁹. In order to meet the QE requirements, a bismuth absorber with a thickness of about 60 μm is needed.

Table 1 - Preliminary absorber requirements.

Energy band	$20 \text{ keV} \leq E \leq 100 \text{ keV}$
ΔE_{FWHM}	40 eV
QE	0.3 @ 60 keV
$T_{\text{operation}}$	50 mK

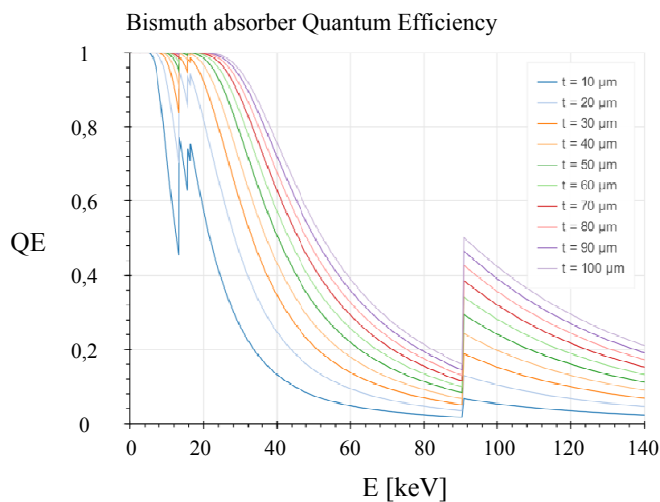


Figure 2 – QE of bismuth absorbers with different thickness, based on X-ray absorption data¹⁹.

3. ELECTROPLATING PROCESS

Electroplating is an electrochemical technology based on the reduction process of metal cations from a suitable solution (electrodeposition bath) to metal. The schematic description of such process is depicted in Figure 3.

By controlling process parameters (applied electric potential, circulating charge, bath composition, fluid-dynamic conditions, bath temperature), it is possible to tune the properties of the electrodeposited layer such as thickness, composition and morphology. It is noteworthy to mention that the choice of the applied potential, according to thermodynamic equilibria of metal/metal cations in bath solution²⁰, is crucial to avoid side reduction processes that are detrimental for the electrodeposition efficiency.

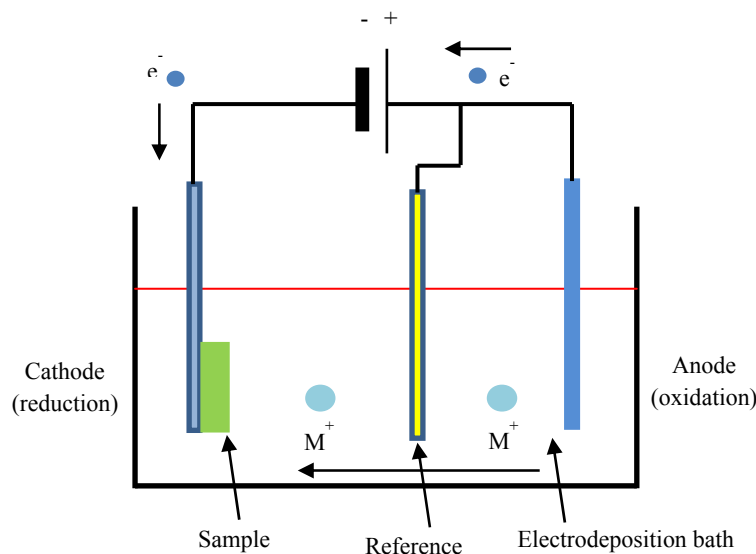


Figure 3 – Schematic description of the electroplating cell.

3.1 Substrates preparation

Suitable substrates were produced from microscope glass slides by cleaving each of them in six samples with dimensions $2.5 \times 1.25 \times 1 \text{ mm}^3$. They were optical grade cleaned by applying the following procedure:

- 1) wash with a mild detergent;
- 2) rins with de-ionized water;
- 3) dry with pure nitrogen;
- 4) degrease in trichloroethylene (TCE) with sonication and successive rinsing with TCE;
- 5) immersion in acetone;
- 6) wash with bi-distilled water with a mild detergent;
- 7) rinse with bi-distilled water;
- 8) final rinse with absolute ethanol.

The cleaned samples were placed into the evaporation chamber of a Varian VT114A electron-beam evaporation system, labelled with “A” in Figure 4, to deposit two metal layers: 20 nm titanium directly on the glass, and 20 nm gold on the previous layer. Final cleaning steps (6 – 7 – 8) and film evaporations were performed in a class 10000 clean room.

3.2 Bismuth electroplating

The experimental setup employed is a three electrodes electrochemical cell connected to a Bio-Logic SA potentiostat. The working electrode (WE) is the metallic substrate where the bismuth layer is electrodeposited, an Ag/AgCl with KCl 3M is the reference electrode, and a DSA (dimensionally stable anode) is the counter electrode (CE). The electroplating cell is placed on a stirring hot plate. The cell setup is shown in Figure 5. The electroplating solution²¹ composition is reported in Table 2. The solution had pH=0.10, measured by a Hanna laboratory pH-meter, and was moderately stirred during the electrodeposition to increase the film uniformity.

Cyclic voltammetry²² is a potention-dynamic method used in analytical chemistry and industrial processes in order to obtain analytical, thermodynamic, kinetic and mechanistic information about the chemical system under investigation. In this method, the WE potential measured with respect to the reference electrode is cyclically scanned in the range from the starting potential to the so called switching potential, and the current flowing between the above electrodes is continuously measured. The scan cycle number is a process parameter.

Cyclic voltammetry curves, reporting the current flowing between the WE and the reference electrode as a function of the applied potential (Figure 6) were recorded before starting the electroplating in order to investigate the useful potential range for the electrodeposition according to the thermodynamic stability region of bismuth in aqueous

solution²⁰. The sweep rate was -2 mV s^{-1} and the electrode potential was scanned starting from OCP (Open circuit potential) to cathodic direction. The lower potential was $\sim -0.1 \text{ V}$ vs. AgCl, higher with respect to the reduction potential of H^+ / H_2 (-0.2 V vs. Ag/AgCl at this pH), to avoid the hydrogen evolution. Fig. 6 shows that the cathodic current starts at $\sim 0 \text{ V}$ vs. Ag/AgCl: this cathodic current can be related to the reduction of Bi^{3+} to Bi leading to the deposition of bismuth layer on gold substrate. This potential is in agreement with that reported in the Pourbaix diagram²⁰: after several electrodeposition attempts, the best morphology of the metallic layer was obtained in the potential range of $-0.04 \leq E_s \leq 0 \text{ V}$ vs. Ag/AgCl reference. A recorded deposition current density diagram $J(t)$ vs. time is shown in Figure 7. The solution pH has to be strictly controlled as for values greater than 0.13 there was white precipitate formation and the deposited film was inconsistent, while for $\text{pH} < 0$ no deposition occurred. The current density affects the layer growth: high values ($J > 15 \text{ mA/cm}^2$) produced tall dendrites, low values ($J < 6 \text{ mA/cm}^2$) produced compact films. The bath temperature strongly influences deposition trend and quality: best results were obtained at room temperature.



Figure 4 – Evaporation beam equipment in the INAF-OAPA XACT facility clean-room.

Table 2 - Electroplating solution composition.

Bismuth nitrate pentahydrate	$\text{Bi}(\text{NO}_3)_3 \cdot \text{H}_2\text{O}$	3.75 g	Honeywell Fluka
Potassium hydroxyde	KOH	3.81 g	Sigma Aldrich
Nitric acid	HNO_3	5.7 ml	J. T. Baker
Glycerol	$\text{CH}_2\text{OHCHOHCH}_2\text{OH}$	6.25 g	Chem Lab
Tartaric acid	$\text{HOOC}(\text{CHOH})_2\text{COOH}$	2.5 g	Chem Lab
Water (bidistilled)	H_2O	50 ml	---

4. RESULTS

Electrodeposited films morphology was observed with a Phenom-world model Phenom ProX SEM, and EDX analyses were performed with the same instrument to evaluate the presence of contaminants. After a process optimization, we obtained a compact bismuth layer, about $67 \mu\text{m}$ thick (Figure 8 a, b, c), with no contaminants detectable by the EDX analysis (Figure 9). Apart the two main peaks, in Figure 9 secondary bismuth peaks can be observed.

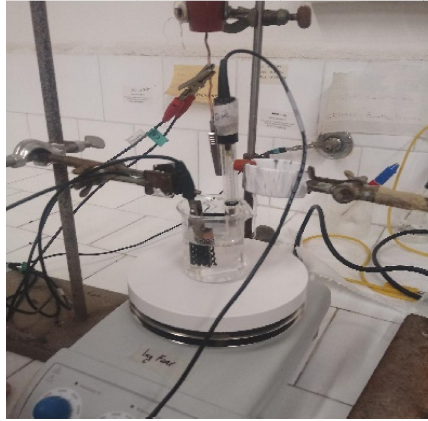


Figure 5 – Experimental setup used for bismuth electroplating.

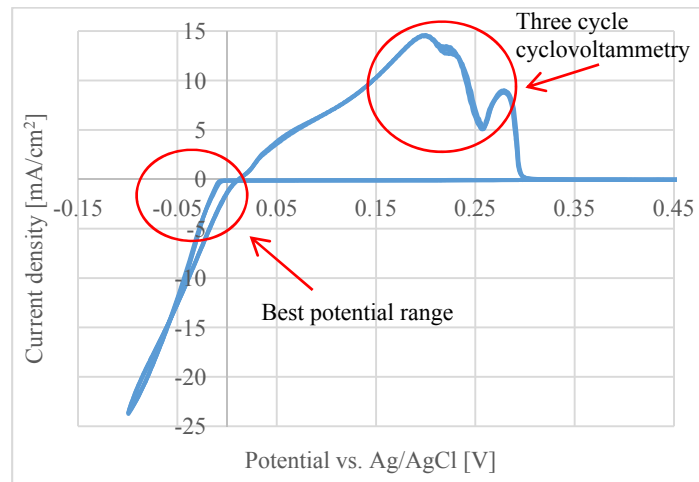


Figure 6 – Three-cycle cyclic voltammetry curve for the bismuth electroplating solution.

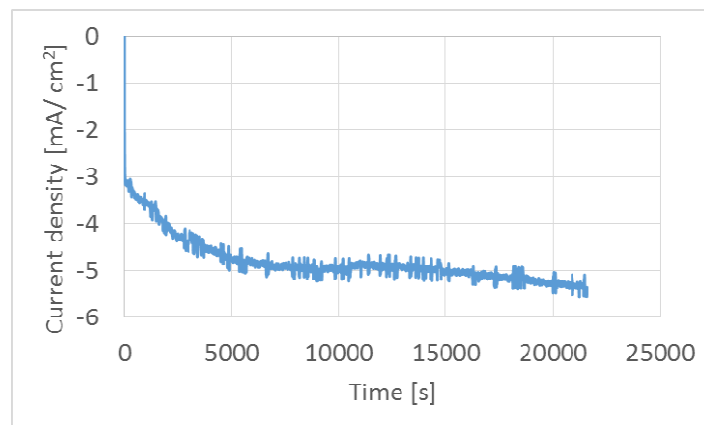


Figure 7 – Plot of the current density $J(t)$ vs. time for a 67 μm thick Bi film deposition.

5. CONCLUSIONS AND WORK PERSPECTIVES

We demonstrated that the reported electroplating process is suitable to grow thick and uniform Bi films. The thickness obtained, $> 60 \mu\text{m}$, meets requirements for fabricating absorbers for a planar array of hard X-ray microcalorimeters. Preliminary X-ray absorption measurements will be performed at INAF-OAPA XACT Laboratory²³ to measure the QE at energy up to 20 keV of absorbers produced with this method; higher energy measurement will be performed later on.

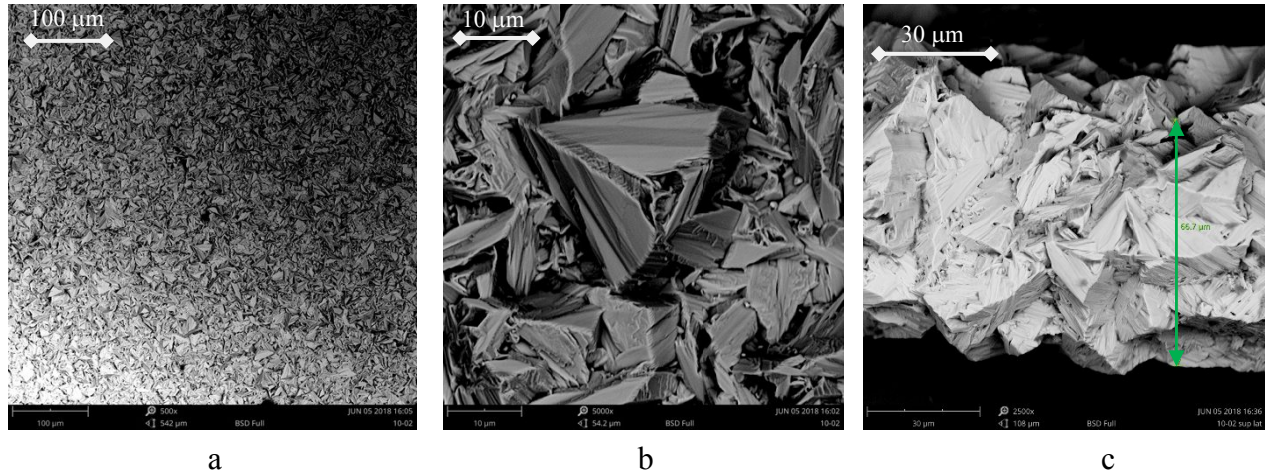


Figure 8 – Electroplated bismuth layer SEM micrographs: low magnification (a); high magnification (b); lateral view with about $67 \mu\text{m}$ measured thickness evidenced (c).

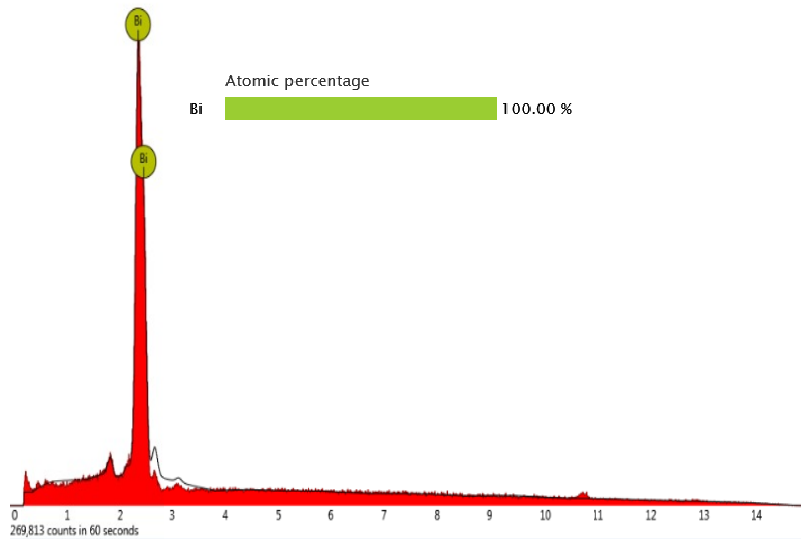


Figure 9 – Electroplated bismuth layer EDX analysis; it can be noted there are only bismuth peaks within the instrument specifications.

6. ACKNOWLEDGMENTS

This research has received funding in the framework of the MISTER-X balloon borne experiment preliminary activities encompassed by the Memorandum of Understanding n. 2016-1-P-O between ASI and INAF. The authors thanks Dr. Lisa Gades at Argonne National Laboratory, Argonne, IL, USA, for helpful discussion.

7. REFERENCES

- [1] S. Krucker et al., "Hard X-ray emission from the solar corona", *The astron. and astrophis. rew.*, 15, 155 – 208, (2008).
- [2] Hudson, H S. et al., "The Hard Solar X-Ray Spectrum Observed from the Third Orbiting Solar Observatory", *Astrophys. J.*, 157, 389-415, (1969).
- [3] Lin R P. et al., "The reuven ramaty high-energy solar spectroscopic imager (RHESSI)", *Solar Phys.*, 210, 3–32, (2002).
- [4] Moseley S. H. et al., "Thermal detectors as x-ray spectrometers", *J. Appl. Phys.* 56, 1257-1262 (1984).
- [5] Silver, E. et al., "High Resolution X-Ray Spectroscopy Using Germanium Microcalorimeters", *Proc.SPIE* 1159, 423-432, (1989).
- [6] Bandler S. et al., "NTD-GE-based microcalorimeter performance", *Nucl. Instr. And Meth. in Physics Research A*, 444, 273-277, (2000).
- [7] Silver, E. et al., "NTD germanium-based microcalorimeters for hard x-ray spectroscopy NTD germanium-based microcalorimeters for hard x-ray spectroscopy", *Proc. SPIE* 4140, 397-401, (2000)
- [8] E. E. Haller, "Isotopically Controlled Semiconductors", *Solid State Comm.*, 133, 693-707, (2005).
- [9] Garai A. et al., "Development of NTD sensors for superconducting bolometer", *J. low temp. phys.*, 184, 609-614 (2016).
- [10] K. Pretzl, "Cryogenic calorimeters in astro and particle physics", *Nucl. instr. and meth. in phys. res. A*, 454, 114 – 127 (2000).
- [11] Yokohama Y. et al., "Improvements of an X-ray microcalorimeter for detecting cosmic rays", *Proc. SPIE Micromachining and Microfabrication*, 4230, 58 - 65 (2000).
- [12] Lo Cicero, U. et al., "Fabrication of Electrical Contacts on Pyramid-Shaped NTD-Ge Microcalorimeters Using Free-Standing Shadow Masks", *J. low temp. phys.*, 167, 541-546 (2012).
- [13] Lo Cicero, U., et al., "Electroplated indium bumps as thermal and electrical connections of NTD-Ge sensors for the fabrication of microcalorimeter arrays", *J. low temp. phys.*, 167, 535-540, (2012).
- [14] Lo Cicero, U. et al., "Planar array technology for the fabrication of germanium X-ray microcalorimeters", *Proc. of IEEE Nuclear Science Symposium Conference Record, NSS'08*, 1789-1792, 2008.
- [15] Lo Cicero, U. et al., "Planar Technology for NDT-Ge X-Ray Microcalorimeters: Absorber Fabrication", *Proc. of AIP Conference*, 1185, 112-114 (2009).
- [16] Jiang S. et al, "Synthesis of bismuth with various morphologies by electrodeposition", *Inorg. Chem. Comm.*, 6, 781 – 785 (2003).
- [17] Corruccini R. J. and Gniewek J. J., [Specific heats and enthalpies of technical solids at low temperatures], US Department of Commerce, National Bureau of Standards, Washington DC, 1 – 6 (1960).
- [18] Kothari L. S. and Tewary V, K., "Calculations on the low temperature specific heat of bismuth", *Phys. lett.*, 6, 248 (1963).
- [19] Henke B. L. et al." X-ray interactions: photoabsorption, scattering, transmission, and reflection at E=50-30000 eV, Z=1-92, *Atomic Data and Nuclear Data Tables*, 54 181-342, (1993).
- [20] Pourbaix M., [Atlas of Electrochemical Equilibria in Aqueous Solutions], Pergamon Press, Oxford, 534-536, 1966.
- [21] Gades L. M. et al., "Development of thick electroplated bismuth absorbers for large collection area hard X-ray transition edge sensors", *IEEE Trans. on applied supercond.*, 27, 2101105 (2017).
- [22] Nicholson R. S., "Theory and Application of Cyclic Voltammetry for Measurement of Electrode Reaction Kinetics", *Anal. Chem.*, 37, 1351-1355, (1965).
- [23] Barbera M, et al., "The Palermo XACT facility: a new 35 m long soft x-ray beam-line for the development and calibration of next-generation x-ray observatories", *PROC. SPIE* 6266, 62663F-1 - 62663F-12, (2006).